



# Quantifying the effects of glacier conduit geometry and recharge on proglacial hydrograph form

M.D. Covington<sup>a,\*</sup>, A.F. Banwell<sup>b,c</sup>, J. Gulley<sup>c,d</sup>, M.O. Saar<sup>e</sup>, I. Willis<sup>b</sup>, C.M. Wicks<sup>f</sup>

<sup>a</sup> Karst Research Institute ZRC SAZU, Postojna, Slovenia

<sup>b</sup> Scott Polar Research Institute, Department of Geography, University of Cambridge, Cambridge, UK

<sup>c</sup> Department of Geology, University Centre in Svalbard, Longyearbyen, Norway

<sup>d</sup> University of Texas Institute for Geophysics, Austin, TX, USA

<sup>e</sup> Department of Geology and Geophysics, University of Minnesota, Minneapolis, MN, USA

<sup>f</sup> Department of Geology and Geophysics, Louisiana State University, Baton Rouge, LA, USA

## ARTICLE INFO

### Article history:

Received 10 June 2011

Received in revised form 28 September 2011

Accepted 10 October 2011

Available online 31 October 2011

This manuscript was handled by Andras Bardossy, Editor-in-Chief, with the assistance of Erwin Zehe, Associate Editor

### Keywords:

Glacier

Hydrograph

Recharge–discharge relations

Karst

Response time

Pipe flow

## SUMMARY

The configuration of glacier hydrological systems is often inferred from proxy data, such as hydrographs, that are collected in proglacial streams. Seasonal changes in the peakedness of hydrographs are thought to reflect changes in the configuration of the subglacial drainage system. However, the amount of information that proglacial hydrographs contain about drainage system configurations depends critically on the degree to which the drainage systems modify recharge hydrographs. If the drainage system does not modify recharge hydrographs, then proglacial hydrographs primarily reflect the recharge conditions produced by supraglacial inputs. Here, we develop a theoretical framework to determine the circumstances under which glacier drainage systems can modify recharge hydrographs and the circumstances under which recharge pulses pass through glaciers unchanged. We address the capability of single conduits, simple arborescent conduit networks, and linked cavity systems to modify diurnal recharge pulses. Simulations of discharge through large sets of such systems demonstrate that, unless large reservoirs or significant constrictions are present, the discharge hydrographs of simple glacial conduit systems are nearly identical to their recharge hydrographs. Conduit systems tend not to modify hydrographs because the changes in storage within englacial and subglacial conduit networks on short time scales are typically small compared to their ability to transmit water. This finding suggests that proglacial hydrographs reflect a variety of factors, including surface melt rate, surface water transfer, and subglacial water transfer. In many cases the influence of subglacial processes may be relatively minor. As a result, the evolution of proglacial hydrographs cannot be used unambiguously to infer changes in the structure or efficiency of englacial or subglacial hydrological systems, without accurate knowledge of the nature of the recharge hydrograph driving the flow.

© 2011 Elsevier B.V. All rights reserved.

## 1. Introduction

The configuration of glacial hydrologic systems exerts a strong control on subglacial water pressure and glacier sliding speeds (Fowler, 1987; Kamb, 1987; Willis, 1995; Mair et al., 2002; Bingham et al., 2003). At the beginning of a melt season, englacial conduits and/or fractures can rapidly deliver supraglacial meltwater to subglacial drainage systems that may be constricted or poorly developed. If meltwater recharge exceeds the hydraulic capacity of the drainage system, water backs up into reservoirs, such as the unfilled portions of conduits, crevasses, and lakes (Boon and Sharp, 2003; Sugiyama et al., 2005). This process increases the hydraulic head in the connected subglacial drainage system and

may result in faster rates of basal glacier motion by reducing effective pressure (Bartholomaus et al., 2008). Continued enlargement of glacier hydrologic systems through wall melting increases hydraulic capacity and allows melt water to be discharged more efficiently, thereby increasing effective pressure and decreasing rates of basal motion.

Since glacial hydrologic systems are often inaccessible, and the ability of geophysical techniques to image hydrologic features decreases as ice thickness increases (Murray et al., 2000; Fountain et al., 2005), much information regarding the structure of subglacial hydrologic systems comes from proxy techniques involving data collected proglacially, such as dye tracing (e.g. Willis et al., 1990; Hock and Hooke, 1993; Nienow et al., 1998; Schuler and Fischer, 2009), geochemical studies (e.g. Tranter et al., 1996; Anderson et al., 2003), and hydrograph/chemograph analyses (e.g. Hannah et al., 1999; Swift et al., 2005; Jobard and Dzikowski,

\* Corresponding author. Tel.: +386 5 700 19 00; fax: +386 5 700 19 99.

E-mail address: [speleophysics@gmail.com](mailto:speleophysics@gmail.com) (M.D. Covington).

2006). Changes in data sets collected at proglacial locations are often used to infer changes in the morphology of the subglacial drainage system such as switches between distributed and channelized flow. Tracer breakthrough curves and hydrographs that are low and broad are frequently inferred to indicate flow in a distributed system whereas sharply peaked dye breakthrough curves and hydrographs are inferred to indicate conduit flow (Nienow et al., 1998; Swift et al., 2005; Jobard and Dzikowski, 2006). Because hydrographs and dye trace breakthrough curves become more peaked as the snowline retreats up-glacier, it is generally thought that the rate of snowpack removal is the dominant control on the timing of the transition from a distributed to a conduit subglacial hydrological system (Nienow et al., 1998; Swift et al., 2005).

However, it is also possible that changes in these proglacial data reflect changes in the rate of delivery of meltwater to conduits as the snowpack retreats. If supraglacial recharge signals pass through glaciers unchanged, then they convey little information about the structure of the englacial or subglacial systems through which they pass. Therefore, correct interpretation of proglacial stream data requires a good understanding of the relative contributions of supraglacial processes (recharge) and the drainage system morphology to proglacial stream outputs (Flowers, 2008; Schuler and Fischer, 2009; Werder et al., 2010a).

While hydrographs, chemographs, and tracer breakthrough curves are all separate entities that potentially carry independent information, accounting for the changes in flow is of primary importance in understanding each of these signals. Recent work has suggested that the shape of dye tracer breakthrough curves can respond to changes in the rate of recharge during the removal of the snowpack (Schuler et al., 2004; Schuler and Fischer, 2009; Werder et al., 2010a; Gulley et al., submitted for publication), and are therefore not a unique indicator of changes in the configuration of the subglacial drainage system. In particular, Gulley et al. (submitted for publication) observed highly dispersed breakthrough curves, which are often interpreted to indicate distributed flow, during low-discharge conditions in a humanly-traversable channelized system. In this paper we investigate the extent to which recharge controls the shape of proglacial hydrographs in simple glacial conduit systems.

A number of studies have used numerical and analytical solutions of various forms of pipe-flow equations to explore the dynamics of glacial conduit and distributed systems (e.g. Röthlisberger, 1972; Spring and Hutter, 1981; Walder and Fowler, 1994; Arnold et al., 1998; Clarke, 1996; Flowers and Clarke, 2002; Flowers, 2008; Schuler and Fischer, 2009; Werder et al., 2010a; Schoof, 2010). Some studies have additionally used these models to examine coupling between conduit and distributed flow systems. In this paper, we examine the conduit system in isolation, using the pipe-flow approach to develop a conceptual and mathematical framework for determining the influence of conduit recharge and conduit geometry on proglacial hydrographs.

In Section 2 we describe a theoretical framework, which employs a hydraulic response time, that was used to study recharge–discharge relations in single karst conduits segments, and in Section 3 we demonstrate that this framework can also be applied to glacial conduits. Section 4 explores recharge–discharge relations in simple single element glacial conduit systems using large simulation sets of conduit elements with geometrical parameters randomly chosen within realistic ranges. In Section 5 we extend the theoretical framework to address simple arborescent and linked-cavity networks. Section 6 includes several example simulations that illustrate the main conclusion of this work, and Section 7 discusses the implications of our results.

## 2. A model for simple karst aquifers

Covington et al. (2009), hereafter denoted C09, used a pipe flow model to explore the relationship between recharge and discharge hydrographs in karst aquifers, delineating regimes in which the discharge hydrographs of karst conduits are controlled by either recharge or conduit geometry. Here, we adapt this model for use in glacier hydrological systems. C09 divided karst aquifers into fundamental elements according to the manner of their response to transient flow. A particular segment of conduit can behave as a full pipe, an open channel, or a reservoir-constriction (Fig. 1). A full pipe conduit is completely filled with water. By conservation of mass, the discharge out of a full pipe is equal to the recharge into it. An open channel is a partially filled conduit much like a surface stream. Since the open channel has a free surface, the volume of water in the system can change and recharge and discharge need not be equal at any given time. The reservoir-constriction is essentially a combination of the previous two elements but behaves in a fundamentally different way. It is composed of a reservoir with a free surface that is drained by a full pipe segment (the constriction). In general, karst aquifers are combinations of these elements that form complex networks. However, analysis of the behavior of single elements provides first-order insight into how a flood wave is altered (if at all) as it propagates through the system. These first-order controls are harder to identify in models of complex systems, because the model parameter space is also correspondingly complex.

The approach in C09 considers two limiting cases. If the recharge function changes very slowly with time, then the conduit system remains near hydraulic equilibrium with slow changes in storage volume, and the recharge and discharge hydrographs are similar (the recharge-dominated limit). Conversely, if the recharge changes rapidly, then the system is thrown out of hydraulic equilibrium, storage changes rapidly, and the discharge hydrograph is different from the recharge hydrograph (the geometry-dominated limit). In order to quantify these limits, we must first define ‘quickly varying’ and ‘slowly varying’ recharge. This is

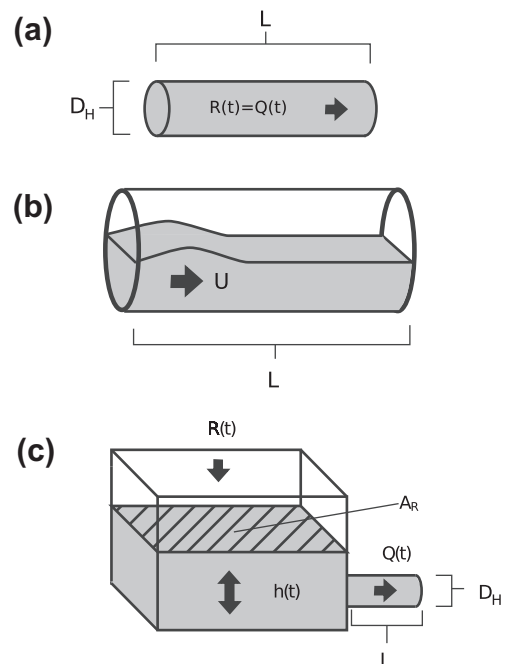


**Fig. 1.** The elements of a conduit network: full pipes (a), open channels (b), and reservoir-constrictions (c). Each element type has a different hydraulic response to a change in recharge, and a different associated response time. Modified from Covington et al. (2009).

accomplished by comparing the time scale of the recharge with the hydraulic response time of a particular conduit element. Using a ratio of these two time scales, C09 define a dimensionless number to characterize conduit hydraulic response:

$$\gamma = \frac{\text{Hydraulic Response Time}}{\text{Recharge Time Scale}} = \frac{\tau}{\sigma}. \quad (1)$$

Using the equations that govern flow through each element type, one can derive hydraulic response times for each (see C09 for details):

$$\tau_{\text{full}} \sim \frac{D_H}{fV_f}, \quad (2)$$

where  $\tau_{\text{full}}$  is the full pipe response time,  $D_H = 4A_c/P_w$  is the conduit hydraulic diameter,  $A_c$  is the cross-sectional area of the conduit,  $P_w$  is the conduit wetted perimeter,  $f$  is the Darcy–Weisbach friction factor, and  $V_f$  is the peak flow velocity.

$$\tau_{\text{open}} = \frac{L}{U}, \quad (3)$$

where  $\tau_{\text{open}}$  is the open channel response time,  $L$  is the conduit length, and  $U$  is the kinematic wave celerity.

$$\tau_{\text{res}} \sim \frac{A_R C_f R_{\text{peak}}}{2gA_c^2}, \quad (4)$$

where  $\tau_{\text{res}}$  is the reservoir-constriction response time,  $A_R$  is the reservoir surface area,  $C_f = 1 + fL/D_H$  is a constant that accounts for energy losses,  $R_{\text{peak}}$  is the peak recharge, and  $g$  is Earth's gravitational acceleration. The equations use hydraulic diameter,  $D_H$ , and cross-sectional area,  $A_c$ , so that the results are generalized for a wide variety of cross-sectional shapes. For circular conduits,  $D_H$  is the physical diameter, and  $A_c = \pi D_H^2/4$ . The derivation of Eq. (4) uses the Darcy–Weisbach equation for pipe flow.

By the reasoning above, we expect cases with large  $\gamma$  to produce significant modification of recharge hydrographs, whereas if  $\gamma$  is small then little modification should occur. To test this hypothesis, and determine critical transition values for  $\gamma$ , i.e.  $\gamma_{\text{crit}}$ , C09 simulated flows through conduits with a wide range of randomly chosen geometries using Gaussian recharge curves with randomly chosen widths,  $\sigma$ .  $\gamma$  was calculated using the response times above and letting the recharge time scale equal  $\sigma$ . This showed that, as expected,  $\gamma$  effectively divides recharge- and geometry-dominated cases. For geometry-dominated cases ( $\gamma \gg \gamma_{\text{crit}} \sim 1$ ), the conduit significantly modifies the recharge hydrograph, and therefore the discharge hydrograph contains significant information about the system. The shape of the hydrograph will be strongly correlated with physical properties of the drainage system, such as reservoir surface areas and constriction diameters, and in some cases it would be possible to estimate these parameters. For recharge-dominated cases ( $\gamma \ll \gamma_{\text{crit}} \sim 1$ ) the discharge hydrographs have nearly identical shapes to the recharge hydrographs and therefore carry much less information about system geometry. Specifically, they only constrain the system properties to be such that the system does not modify hydrographs, leaving open a wide range of possible flow system geometries.

In general, the results for karst aquifers suggested that conduits with geometrical parameters that are likely to occur in nature are unlikely to modify the shape of recharge hydrographs unless there are significant constrictions causing water to back up into large reservoirs. Full pipes and open channels do not typically modify hydrographs, and reservoir-constrictions only do so in some cases. Since reservoir-constrictions are the only type of simple hydraulic element likely to modify hydrographs, we limit our study of single glacial conduit elements to reservoir-constrictions.

### 3. Application of the model to glacial conduit systems

Hydraulically speaking, most elements of glacier conduit systems are analogous to karst conduit networks, with the flow occurring through elements that can be mathematically represented as full pipes, open channels, and reservoirs of various kinds (Clarke, 1996). Because of this analogy, and to simplify the discussion in this paper, we use the word “conduit” to include any aspect of the glacier hydrological system that may be hydraulically represented with pipe flow equations, which includes linked cavities, not just the traditional “conduit” as defined by Shreve (1972) and Röthlisberger (1972). For the models developed here, ‘recharge’ is defined as the flow of water into the conduit system, usually via moulins or crevasses.

A key difference between karst and glacial hydrological systems is that the glacial system can change size or configuration within days or even hours as a result of creep or melt. Since the time scales over which glacial conduits change are close to the time scales of recharge events, we must assess if and when these changing geometries can affect recharge–discharge relationships. Importantly, the reservoir-constriction response time is sensitively dependent on constriction diameter, with  $\tau_{\text{res}} \propto 1/D_H^5$ . Therefore, if conduit diameters change too quickly during a recharge event then the response time given by Eq. (4), which is derived using static conduit geometries, will not apply for the duration of the event.

To test whether melt and creep significantly influence recharge–discharge relations in a variety of conditions, we run four sets of simulations. The first set is run with conduit geometries fixed over time, as in the karst case above. For the other three simulation sets, we allow the conduit diameters to change over time with melt and creep, examining three different choices in ice thickness.

Flow through a reservoir-constriction is governed by the equations

$$\frac{dh}{dt} = \frac{R - Q}{A_R} \quad (5a)$$

$$Q = A_c \sqrt{\frac{2gh}{C_f}}, \quad (5b)$$

where  $Q$  is the volumetric discharge,  $R$  is the recharge, and  $h$  is the depth of water in the reservoir (Eqs. (24) and (25) in Covington et al., 2009). For the simulations here, we use Gaussian recharge curves with width,  $\sigma$ , and a peak,  $R_{\text{peak}}$ . The curves are truncated at a base flow value  $R_{\text{base}}$ . We use the maximum of the normalized cross-correlation between recharge and discharge hydrographs ( $XC_{\text{max}}$ ) to quantify the extent to which the systems modify hydrographs. By definition, if the recharge and discharge hydrographs have the same shape then the normalized cross-correlation coefficient is one.

For the simulations that include melt and creep we utilize

$$\frac{dA_c}{dt} = \frac{f\rho_w}{8\rho_i L_f} \frac{P_{\text{wet}} Q^3}{A_c^3} - 2 \left( \frac{1}{nB} \right)^n A_c (P_i - P_w) |P_i - P_w|^{(n-1)}, \quad (6)$$

where  $\rho_w$  and  $\rho_i$  are the density of water and ice, respectively,  $L_f$  is the latent heat of fusion of water,  $P_{\text{wet}}$  is the conduit wetted perimeter,  $n$  is the ice flow law exponent,  $B$  is the Arrhenius parameter, and  $P_w$  and  $P_i$  are the conduit water pressure and ice overburden, respectively. The equations describing melt and creep are derived in Spring and Hutter (1981), as used in the model by Arnold et al. (1998). This simplified formulation assumes that material derivatives of temperature are negligible compared with other energy terms, which is an oversimplification that can lead to errors in the application of a proper frictional factor (Clarke, 2003). Consequently, we sample a wide range of frictional factors in the simulations below. This approach is mathematically identical to the

**Table 1**

Values of constants used in the calculations of melt and creep.

Parameter	Value	Units
$\rho_w$	1000	$\text{kg m}^{-3}$
$\rho_i$	900	$\text{kg m}^{-3}$
$L_f$	$3.34 \times 10^5$	$\text{J kg}^{-1}$
$n$	3	(unitless)
$B$	$5.8 \times 10^7$	$\text{N m}^{-2} \text{s}^{-n}$

“Röthlisberger resistor” described by Clarke (1996). The values we chose for the constants in Eq. (6) are displayed in Table 1. For simplicity, we use circular cross-sections.

To test whether  $\gamma$  effectively characterizes the extent to which hydrographs are determined by recharge versus flow-element geometry, we numerically integrate Eqs. (5) and (6) for many randomly chosen geometrical and recharge parameters and plot  $\gamma$  versus  $XC_{\max}$  for each parameter set. Numerical integration is accomplished using the ODEPACK solver *lsode* (Hindmarsh and ODEPACK, 1983) as implemented in Octave (<http://www.gnu.org/software/octave/>). For each simulation we randomly choose geometrical and recharge parameters uniformly in log space from the ranges in Table 2. These ranges are chosen to cover the majority of the potential values of these parameters in nature. Parameter choices are further constrained such that the base flow reservoir depth is at least twice the diameter of the conduit draining the reservoir. This constraint assures that the conduit remains submerged during the simulation, otherwise it could enter the open channel regime and Eq. (5) would no longer apply. For simulations including creep and melt, peak reservoir depths are required to be less than the ice thickness, to prevent the generation of unrealistically-high water elevations at the input point. Recharge parameters are specified by first choosing random values for  $\sigma$  and base flow,  $R_{\text{base}}$ , and then choosing a random multiplying factor to calculate  $R_{\text{peak}}$ .

The dimensionless number,  $\gamma$ , and the maximum of the normalized cross-correlation,  $XC_{\max}$ , are shown in Fig. 2 for 500 randomly chosen cases each for static conduits (a) and evolving conduits beneath 100 m (b), 500 m (c), and 1000 m (d) of ice. For the static case,  $\gamma \sim 1$  effectively separates recharge- and geometry-dominated cases. This result is expected, since the static conduits are directly analogous to those for karstic reservoir-constrictions as described in Section 2. We use the static case as a reference point to examine departures as melt and creep closure are included in the analysis.

A fixed value of constriction hydraulic diameter,  $D_H$ , must be assigned in order to calculate  $\gamma$ . However, when melt and creep are included, constriction diameters are a function of time. To account for this effect, we use the average diameter during the simulation in order to calculate  $\gamma$ . Departures from the static model can be observed by examining whether the evolving conduit simulations produce significant scatter outside the envelope of values seen for the static model. Melt and creep have opposite effects on the

**Table 2**

Ranges from which parameters were uniformly drawn in log space for simulations of glacial reservoir-constriction elements (Fig. 1c).

Parameter	Min	Max	Units
$D_H$	0.01	5	m
$L$	100	10,000	m
$f$	0.01	0.5	(unitless)
$\sigma$	3	6	h
$R_{\text{peak}}/R_{\text{base}}$	2	10	(unitless)
$R_{\text{base}}$	0.01	10	$\text{m}^3 \text{s}^{-1}$
$A_R$	1.0	$10^6$	$\text{m}^2$

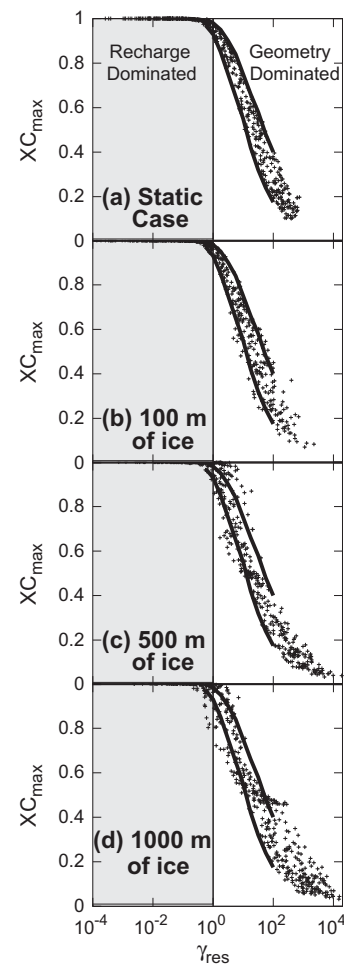


**Fig. 2.** The dimensionless number,  $\gamma$ , versus the maximum of the normalized cross-correlation of the recharge and discharge hydrographs,  $XC_{\max}$ , calculated from 500 randomly chosen glacial reservoir-constrictions. For the top panel (a), conduits remain static throughout each simulation, and  $\gamma$  divides the recharge- and geometry-dominated responses with a critical value  $\gamma_{\text{crit}} \sim 1$ . In all panels, the thick black lines show an approximate envelope around the relationship for static conduits (a). In panels b–d, conduit diameters change via melt and creep with three choices of ice thickness. Scatter outside the envelope of the static solution is indicative of the effects of melt (above the envelope) and creep (below the envelope) but is sufficiently small to allow use of  $\gamma$  in characterizing glacial conduit systems up to an ice thickness of  $\sim 1000$  m.

evolution of  $\gamma$  over time. Melt increases the constriction diameter, which decreases system response time and, therefore, produces more recharge-controlled responses than would be expected for the calculated value of  $\gamma$ . This results in model outputs that plot above the static envelope in Fig. 2. Creep decreases the constriction diameter, therefore increasing response time results in model outputs that plot below the static envelope in Fig. 2. If the conduit geometry changes too much during a recharge pulse, then  $\gamma$  will no longer provide a useful delineation of recharge- and geometry-dominated cases.

The results of the evolving conduit simulations are shown in Fig. 2b–d. For an ice thickness of 100 m, the model performs quite well, with little scatter outside the static envelope. At ice thicknesses of 500 and 1000 m, the dynamics of both melt and creep play a role, producing some scatter above and below the envelope. However, the overall relation still holds. The transition region between recharge and geometry-dominated responses is broadened for larger ice thicknesses, but this does not significantly affect the results of the analysis developed here. For ice thicknesses



greater than 1000 m the will break down as the scatter around transitional cases ( $\gamma \sim 1$ ) gradually increases. Since, for all ice thicknesses examined,  $\gamma$  remains a strong indicator of hydrograph modification (Fig. 2), we conclude that, for the range of parameters studied, melt and creep do not significantly influence the hydraulic response time of a reservoir-constriction over diurnal time scales. While hydraulic response time can vary during a melt pulse, this variation is sufficiently small that comparison of the recharge time scale with a hydraulic response time calculated using the time-averaged diameter of a conduit allows an accurate prediction of the strength of the correlation between recharge and discharge. However, cases with  $\gamma \sim 1$  should be treated with care, as the classification of recharge–discharge behavior using  $\gamma$  in this neighborhood is unambiguous, and some cases will be incorrectly classified. If a particular case with  $\gamma \sim 1$  is important then its recharge–discharge behavior could be examined through a set of simulations with different recharge time scales. These simulations would demonstrate whether  $\gamma$  remains useful, and if so, whether a different transitional value of  $\gamma$  should be used.

#### 4. Characterization of single element responses to transient flow using $\gamma$

To derive some general rules about how various types of glacial drainage elements will affect hydrographs, we divide glacial reservoir-constrictions into three types: conduits, crevasses, and lakes. Conduit type reservoir-constrictions are defined as a conduit that passes from a less-constricted open channel portion into a constricted segment of full-pipe conduit (Fig. 3a). This might be expected to occur, for example, late in the melt season when conduits near the glacier bed have experienced more creep closure than conduits near the glacier surface. Crevasse (Fig. 3b) and lake (Fig. 3c) type reservoir-constrictions are water-filled reservoirs at, or near, the glacier surface that are drained by submerged conduits. We choose a division between crevasse and lake reservoirs based solely on reservoir surface area, where crevasse reservoirs are those that have surface areas less than 100 m<sup>2</sup> and lakes have surface areas greater than 100 m<sup>2</sup>. While this division is somewhat arbitrary, as some crevasses can have surface areas that are larger than 100 m<sup>2</sup>, crevasse and lake are concise labels for these regions of the parameter space.

To explore the circumstances under which proglacial discharge hydrographs contain information about conduit geometry, we simulate discharges from numerous conduit systems. As above, we use Gaussian recharge curves, truncated by a baseflow,  $R_{\text{base}}$ , and we calculate  $\gamma$  and  $XC_{\text{max}}$  for each case, taking the recharge time scale to be the width of the Gaussian pulse,  $\sigma$ . Our simulations include melt and creep and assume a circular conduit cross section. For each of the reservoir-constriction types we simulate 500 cases with geometrical and recharge parameters chosen randomly from uniform distributions in log space within the ranges given in Table 3. These ranges are chosen to represent the likely range of glacier properties.

For conduit type reservoir-constrictions, first a constriction size,  $D_H$ , is chosen and the constriction cross-sectional area calculated. Then a random multiplying factor between 2 and 50 is used to choose an area for the unconstricted portion of the conduit represented by the reservoir surface area,  $A_{R,\text{conduit}}$ . For the crevasse and lake type systems, all parameters are selected randomly from the same ranges except for the reservoir surface area, which for crevasses ranges from 1 m<sup>2</sup> to 100 m<sup>2</sup>, and for lakes from 100 m<sup>2</sup> to 1 km<sup>2</sup>. For all simulations  $\sigma$  is chosen within a range to represent diurnal pulses of melt water.

The results of these simulations, shown in Fig. 4, are given as the maximum of the normalized cross-correlation of recharge and discharge,  $XC_{\text{max}}$ , versus  $\gamma$ , the ratio of the reservoir-constriction hydraulic response time (Eq. (4)) and the recharge time scale,  $\sigma$ . Histograms at the bottom of the figure indicate the distribution of  $\gamma$  values for each type of reservoir-constriction. For  $\gamma < 1$  the

**Table 3**

Ranges from which parameters were uniformly drawn in log space for simulations of the three glacial reservoir-constriction types depicted in Fig. 3.

Parameter	Min	Max	Units
$D_H$	0.01	5	m
$L$	100	10,000	m
$f$	0.01	0.5	(unitless)
$\sigma$	3	6	h
$R_{\text{peak}}/R_{\text{base}}$	2	10	(unitless)
$R_{\text{base}}$	0.01	10	m <sup>3</sup> s <sup>-1</sup>
$A_{R,\text{conduit}}/A_c$	2	50	(unitless)
$A_{R,\text{crevasse}}$	1	100	m <sup>2</sup>
$A_{R,\text{lake}}$	100	10 <sup>6</sup>	m <sup>2</sup>

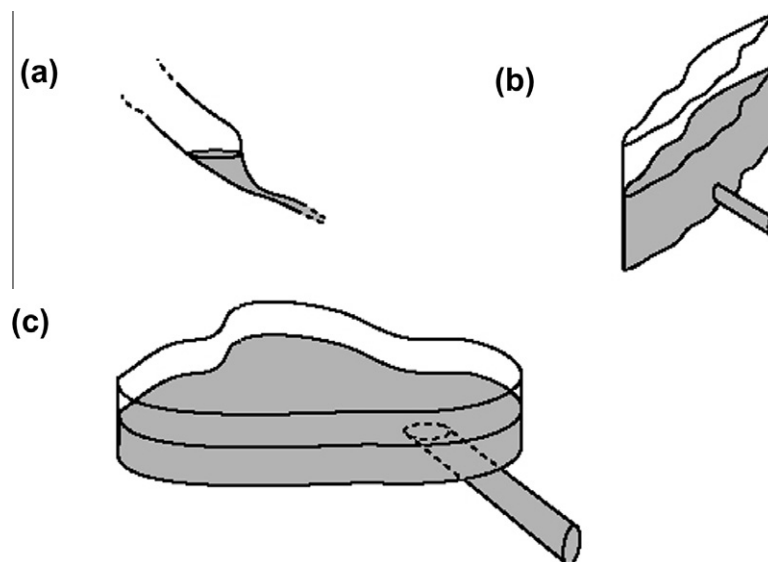


**Fig. 3.** Sketch of the three reservoir-constriction types found in glaciers: (a) conduits, (b) crevasses, and (c) lakes.

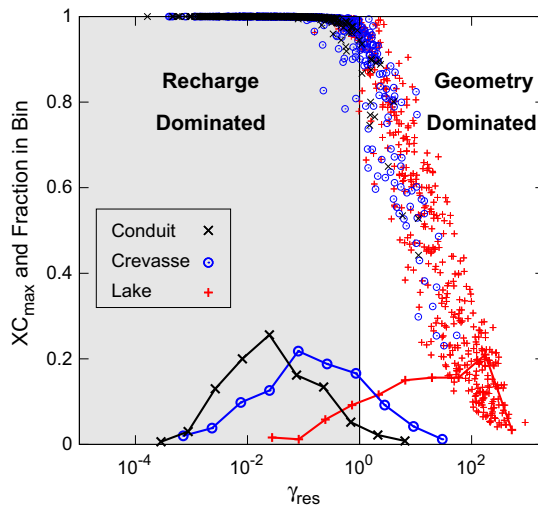


**Fig. 4.** Symbols depict the distribution of the maximum of the cross-correlation between recharge and discharge ( $XC_{\max}$ ) versus the dimensionless number,  $\gamma_{\text{res}}$ , for the randomly chosen glacial reservoir-constriction parameters (Table 3). Conduit types are shown in black x's, crevasse types in blue circles, and lake types in red crosses. Solid lines depict histograms of the distribution of  $\gamma_{\text{res}}$  for each of the reservoir-constriction types, using the same color scheme. The recharge- and geometry-dominated regimes delineate the discharge hydrographs that are either determined solely by the recharge hydrographs or are a strong function of system geometry.

reservoir-constriction produces little modification of the recharge hydrograph and we describe the system behavior as recharge-dominated. For  $\gamma > 1$  the system modifies the recharge hydrograph, and we describe the system behavior as geometry-dominated.

The conduit reservoir-constrictions largely show identical recharge and discharge hydrographs ( $XC_{\max} \sim 1$ ), and lie primarily in the recharge-dominated regime. Crevasse responses are also primarily recharge-dominated, whereas lakes generally have geometry-dominated responses, as indicated by significantly altered hydrographs ( $XC_{\max} < 1$ ) in Fig. 4. While crevasse responses are generally recharge-dominated, and lake responses are generally geometry-dominated, the distribution of each type has a

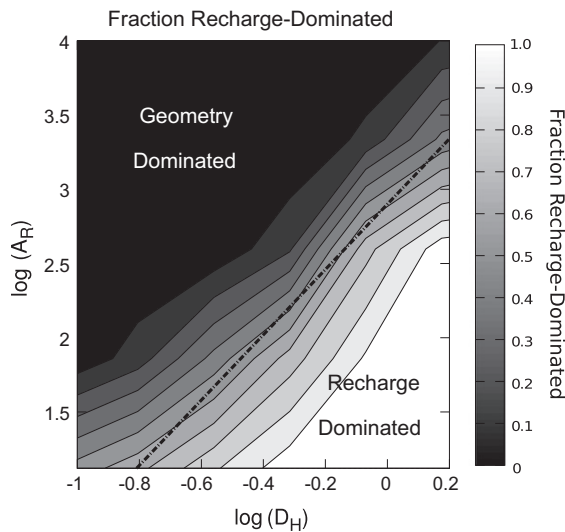


**Fig. 5.** Fraction of stacked lake-type and crevasse-type reservoir-constriction simulations that are recharge dominated as a function of constriction hydraulic diameter,  $D_H$ , and reservoir surface area,  $A_R$ . Gray-scale indicates the fraction of simulations that are recharge-dominated in each bin, with white indicating all cases are recharge-dominated. The dashed line depicts an approximate division between recharge- and geometry-dominated cases (Eq. (7)).

significant tail into the opposite regime. Therefore, we look in more detail at the distribution of  $\gamma$  for each case as a function of other parameters.

Since constriction diameter,  $D_H$ , and reservoir surface area,  $A_R$ , are two of the most important parameters in determining the way a reservoir-constriction will respond, we stack the crevasse- and lake-type simulations and plot a 2D density function of the fraction that are recharge dominated ( $\gamma < 1$ ) as a function of  $D_H$  and  $A_R$  (Fig. 5). From this plot the combined effects of the two parameters can be seen. As a general rule, for the parameter ranges explored here, we can define a dividing line below which most systems (>50%) are recharge-dominated,

$$\log(A_R) \lesssim 2.2 \log(D_H) + 2.9. \quad (7)$$

If a given choice of constriction diameter and reservoir surface area falls well above or below this line, then we can be fairly confident that it is geometry- or recharge-dominated, respectively. The range of  $D_H$  depicted in this figure is smaller than the range from which we are drawing cases,  $0.1 \text{ m} < D_H < 5 \text{ m}$ . This is because the parameter space is poorly sampled for  $D_H > 2 \text{ m}$ , a result of our

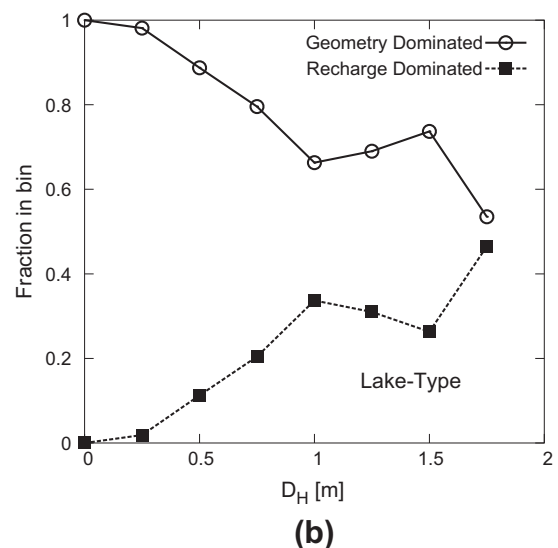
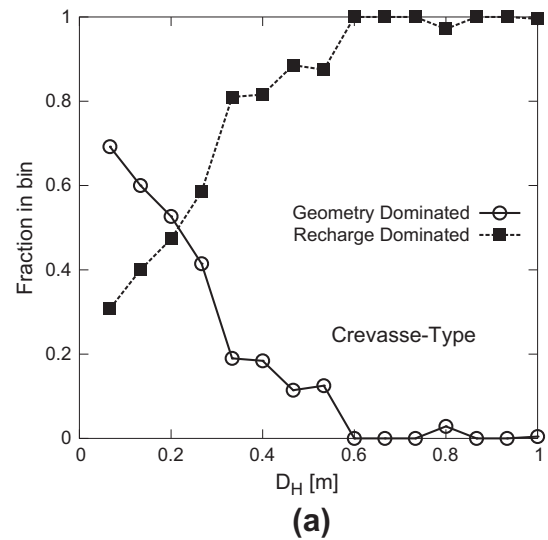


**Fig. 6.** Histograms of the percentage of recharge- and geometry-dominated cases as a function of constriction hydraulic diameter,  $D_H$ , for (a) crevasse-type and (b) lake-type reservoir-constrictions.

constraint that the base flow discharge is sufficient to maintain full pipe flow within the constriction. Essentially, the range of recharge values we have chosen rarely produces pipe full conditions in conduits larger than this diameter.

As would be expected from the functional dependence of hydraulic response time (Eq. (4)), and as is seen in Eq. (7), the parameter that most strongly governs response is the diameter of the constriction. Therefore, we look separately at the behavior of the crevasse and lake cases as a function of constriction diameter. A histogram of the fraction of crevasse cases that are recharge- and geometry-dominated as a function of the hydraulic diameter of the constriction (Fig. 6a) shows that  $D_H \sim 0.2$  m is a critical value below which most cases are geometry-dominated and above which most cases are recharge-dominated. The conclusion for lake cases is not as clear-cut. While most cases are geometry-dominated, a significant percentage of cases with  $D_H > 0.75$  m are recharge-dominated (Fig. 6b).

## 5. Behavior of conduit networks

The analysis so far has focused on the hydraulic behavior of single segments of a glacial conduit network. However, only a small subset of glacial conduit systems can be realistically represented by a single conduit. Most glacial conduit systems consist of networks of open channels, full pipes, and reservoir-constrictions. In the following sections, we examine how the results for single-element systems may also be extended to more complex systems.

### 5.1. Arborescent systems and hydraulic damming

Dye trace studies confirm that supraglacial meltwater in most glaciers sinks at multiple places (crevasses and moulins) on the glacier surface and emerges at one or a small number of resurgences at the glacier snout (e.g. Willis et al., 1990; Nienow et al., 1998). One of the most significant limitations of the single-element model above is that it does not include any of the effects that might result from interactions between conduit segments with separate inputs. For example, dye tracing data suggest that hydraulic damming can

occur, where one conduit reduces or reverses the flow of an infeeder (Smart, 1990; Fountain, 1993; Nienow et al., 1996; Schuler and Fischer, 2009; Werder et al., 2010b). The potential effects of these types of processes on recharge–discharge relations are not accounted for in the preceding single-element analysis.

In order to understand the effects of junctions on hydrographs, it is useful to break down the analysis into two types of qualitatively distinct junction behavior, open channel and full pipe (Fig. 7). A given glacial conduit network will likely transition back and forth between these states. First, we consider arborescent systems of open channels. Open channel networks appear to be a common drainage configuration in thin, cold-based glaciers or polythermal glaciers that lack significant crevassing (Gulley et al., 2009a,b). Such glaciers are common in the high arctic. Extensive, long-lived open channel systems are probably rare in glacier conduit systems under thicker ice as they would quickly be closed due to creep. If we only consider the behavior of junctions of open channels, then, by definition, the increase in hydraulic head at a junction is limited by the height of the conduit at that junction (larger increases in hydraulic head will result in full pipe flow which is treated below). In most subglacial conduits, heights will be a few meters or less. Since infeeding conduits will typically ascend that elevation over a fairly short distance, only a small portion of the infeeding conduit could be influenced by junction effects during open channel flow (Fig. 7a). Therefore, hydraulic interactions at open channel junctions are unlikely to have a significant effect on system hydrographs.

However, even with open channels, the inclusion of multiple recharge points presents a new complexity. The proglacial hydrograph will be a sum of hydrographs from different recharge points, each of which will have a distinct lag time between the recharge point and the response of the proglacial hydrograph. Therefore, the more complex the network, and, specifically, the larger the range of lag times from different recharge points, the more likely it is that proglacial hydrographs will contain features such as smeared peaks or multiple peaks as recharge from different locations reaches the discharge point at different times. Therefore, for arborescent open channel networks, the network geometry will influence the proglacial hydrograph form, but primarily in the sense of adding multiple recharge hydrographs at different times. As hydrographs pass through each individual segment of the system, little modification occurs.

If the system contains networks of full pipes, then junction effects become more prevalent, since the head at a junction can be increased to large values (near flotation), and potentially even cause a tributary to reverse flow along its entire length and interact

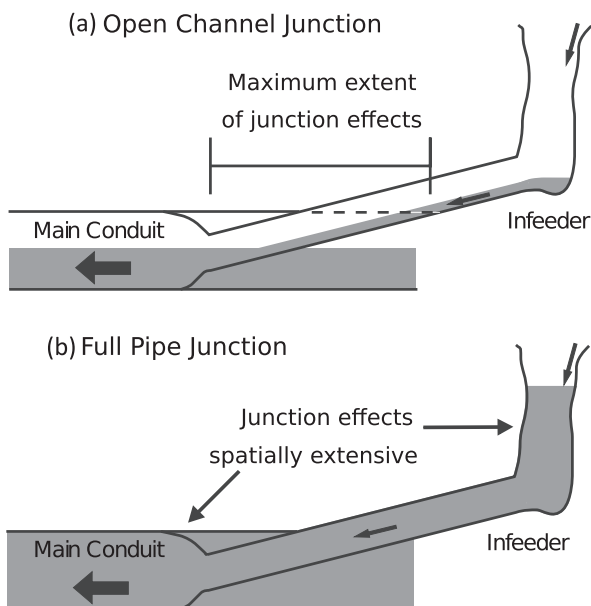


**Fig. 7.** Two types of junction behavior, open channel (a) and full pipe (b). Hydraulic effects of junctions of open channels only influence a limited portion of the infeeding conduit, whereas pressure changes at full pipe junctions can propagate over large distances, potentially as far as surface reservoirs.

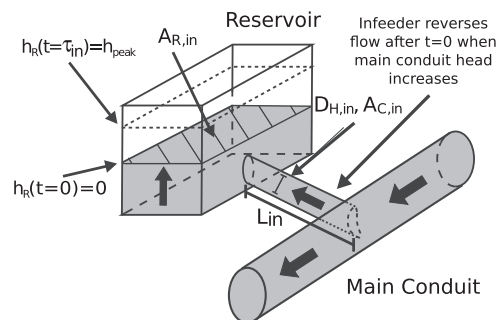


**Fig. 8.** The simplified model of interactions between a main conduit and infeeder used to calculate the hydraulic response time,  $\tau_{in}$ , of an infeeder to pressure changes in the main conduit. We employ a model of a full pipe infeeder that is connected to a reservoir at the glacier surface, and treat the main conduit as a changing head boundary. The response time of the infeeder ( $\tau_{in}$ ) is the time required for the reservoir to fill to an equilibrium depth after an instantaneous change in head in the main conduit.

with reservoirs near the surface (Fig. 7b). In order for a conduit system to alter the recharge hydrographs, the volume of water in the system must change over time via the filling or draining of reservoirs. Therefore, without loss of generality, we can consider various arrangements of connected reservoir–constrictions.

As a first extension of the single-element model, we analyze a system where a main full-pipe conduit is linked to an infeeding conduit connected to a reservoir, such as a crevasse, near the glacier surface (Fig. 8). The hydraulic response time approach can be utilized to study this system as well. Since the infeeder is more likely to reverse if it is carrying a smaller discharge than the main conduit, we consider the response of an infeeder with zero recharge. This simplifies the analysis and is an extreme case that should maximize the effect of the junction dynamics on the discharge hydrograph. In order to derive a response time, we examine the behavior when the hydraulic head in the main conduit suddenly increases, as in the introduction of a pulse of melt water. When the junction head increases, water flows up the infeeder and into the upstream reservoir. The response time of this system is the amount of time that it takes for the reservoir to fill to a high-enough elevation to halt the upstream flow of water in the infeeder. After this point, flow in the main conduit will no longer be diverted up the infeeder.

The system described is governed by a form of the Darcy–Weisbach equation,

$$Q_{in}(t) = A_{c,in} \sqrt{\frac{2g}{C_{f,in}}} (h_c - h_R(t)), \quad (8)$$

which is valid for  $h_c > h_R$ , combined with a continuity equation for the reservoir,

$$\frac{dh_R}{dt} = \frac{Q_{in}(t)}{A_{R,in}}, \quad (9)$$

where  $Q_{in}$  is the upstream flow in the infeeder,  $C_{f,in} = 1 + f_{in}L_{in}/D_{in}$ ,  $A_{c,in}$ ,  $f_{in}$ ,  $L_{in}$ , and  $D_{in}$  are the cross-sectional area, Darcy–Weisbach friction factor, length, and hydraulic diameter of the infeeder conduit, respectively,  $h_c$  and  $h_R$  are the hydraulic heads in the main conduit and infeeding reservoir, respectively, and  $A_{R,in}$  is the surface area of the infeeder reservoir. Assuming a sudden increase in the main conduit hydraulic head from zero to  $h_{peak}$ , Eqs. (8) and (9) can be combined and integrated to derive the reservoir filling time,

$$\tau_{in} = \frac{A_{R,in}}{A_{c,in}} \sqrt{\frac{2C_{f,in}h_{peak}}{g}}. \quad (10)$$

$\tau_{in}$  is an upper limit to the response time, which would be somewhat shorter in the case of recharge entering the infeeding reservoir from the surface. Analogous to our single-element systems, we may define a dimensionless number that characterizes the influence of a given infeeder on recharge–discharge relations,

$$\gamma_{in} = \tau_{in}/\sigma. \quad (11)$$

If  $\gamma_{in} \ll 1$  for a given infeeder, then interactions between that infeeder and the main conduit will have little influence on the discharge hydrograph from the main conduit. This results because, when  $\gamma_{in} \ll 1$ , the reservoir fills quickly, and the system is close to equilibrium at all times during the recharge event, meaning that at all times recharge and discharge are approximately equal. However, unlike single elements there is a second condition required in order for a junction interaction to appreciably influence system discharge. The amount of water reversing up the infeeder must be a significant percentage of the discharge through the main conduit. This additional constraint is significant, since examination of Eqs. (8) and (10) shows that many means of increasing response time (e.g. decreasing  $D_{in}$  or increasing  $L_{in}$  or  $f_{in}$ ) also would

decrease any potential back-flow into the infeeder. Thus, large, open infeeders, which could divert a large amount of the flow, will tend to respond quickly, whereas infeeders with longer response times will tend to also have less capacity to divert water.

An example case gives us an idea of typical infeeder response times. For an infeeder with a circular cross-section, where  $D_{in} = 1$  m,  $L_{in} = 1000$  m,  $A_{R,in} = 100$  m<sup>2</sup>, and  $f_{in} = 0.05$ , and if we allow diurnal head variations of 30 m ( $h_{peak} = 30$  m), then the infeeder response time  $\tau_{in} = 0.6$  h. Therefore, even with a relatively large reservoir surface area, fairly large variations in head, and a kilometer-long connecting conduit, this infeeder can equilibrate quickly compared to the time scale of diurnal melt pulses. The infeeder response time is most sensitive to changes in  $D_{in}$ , with  $\tau_{in} \propto D_{in}^{-5/2}$ , and reservoir surface area, with  $\tau_{in} \propto A_{R,in}$ . With the example parameters above, reducing the infeeder diameter to  $D_{in} = 0.5$  m results in a response time of 3.5 h. At this point, the infeeder response time approaches the time scale of diurnal fluctuations, however, since  $Q_{in} \propto D_{in}^{5/2}$ , the flow capacity of the infeeder is also significantly reduced.

To illustrate the principle of infeeder response time, and its influence on recharge–discharge relations, we run two example simulations, one where  $\gamma_{in}$  is small, and one where  $\gamma_{in}$  is large. Each simulation includes a main conduit fed by a reservoir and a smaller infeeder conduit that joins at some distance along the main conduit and is also fed by a reservoir (Fig. 9). For both cases, the main conduit is recharged at a base rate of 2.0 m<sup>3</sup> s<sup>−1</sup> and then fed with a Gaussian melt pulse with a peak of 6.0 m<sup>3</sup> s<sup>−1</sup> and a width of 5 h. This factor of three increase in recharge is roughly comparable to observed proglacial hydrographs during periods with high peaks (Swift et al., 2005). The recharge,  $R_m$ , enters the main conduit via a reservoir with a surface area of  $A_{R,m} = 10$  m<sup>2</sup>, which is chosen to be small so that the main flow path does not alter the recharge signal. The main conduit flows for 2 km,  $L_{m,1}$ , before reaching the junction with the infeeder, and then flows another kilometer,  $L_{m,2}$ , to the ultimate discharge point. The infeeder is recharged at a base rate of 0.3 m<sup>3</sup> s<sup>−1</sup> and then fed with a Gaussian melt pulse with a peak of 1.0 m<sup>3</sup> s<sup>−1</sup> and a width of  $\sigma = 4$  h. To avoid any possible sensitive dependence of the results on the synchronization of inputs, the infeeder recharge is lagged 2 h behind the main conduit

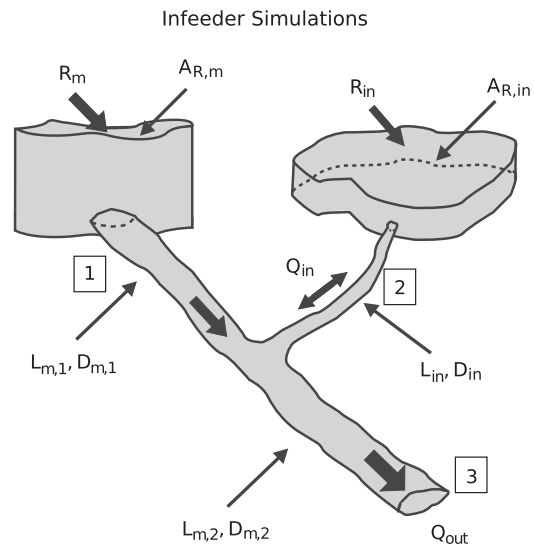


**Fig. 9.** A schematic of the simulations used to illustrate the effect of infeeder response time. The main conduit is fed by a small reservoir (crevasse), with  $A_{R,m} = 10$  m<sup>2</sup>, and the infeeding conduit has a larger reservoir (lake) with surface area  $A_{R,in}$ . The two example simulations differ only in the value of  $A_{R,in}$ , which is set to 100 m<sup>2</sup> for the first simulation and 5000 m<sup>2</sup> for the second. Numbered labels depict locations of flow measurements plotted in Fig. 10.



recharge and the widths of the Gaussian pulses are slightly different. The infeeder is recharged via a reservoir with a surface area of  $A_{R,in} = 100 \text{ m}^2$ , and we have set  $L_{in} = 1000 \text{ m}$  and  $f_{in} = 0.05$ . Ice thickness is assumed to be a constant  $250 \text{ m}$ .

As a result of the continuity equation at the junction, the set of equations for the system is differential–algebraic, and we use the *daspk* solver implemented in Octave. We begin the simulation by running base flow recharges for  $100 \text{ h}$ , which allows the conduit diameters to reach equilibrium values. The resulting main conduit equilibrium diameter is  $D_{m,1} = 0.98 \text{ m}$  above the junction and  $D_{m,2} = 1.02 \text{ m}$  below. The equilibrium infeeder diameter is  $D_{in} = 0.47 \text{ m}$  and  $A_{R,in} = 100 \text{ m}^2$ , resulting in a system roughly equivalent to the one for which we calculated an infeeder response time of  $3.5 \text{ h}$  above.

Hydrographs of discharge through the upper main conduit and the infeeder are shown in Fig. 10a. The increase in head at the junction, which occurs before any increase in recharge in the infeeder, slows, and even briefly reverses, the flow in the infeeder. This hydraulic damping is likely to have an important influence on dye tracer results for tracers injected into such an infeeder (c.f. Nienow et al., 1996; Schuler and Fischer, 2009; Werder et al., 2010b). However, as expected from the time scale analysis above, this system produces discharge hydrographs that are quite similar in shape to the sum of the two recharge hydrographs (Fig. 10b), with a large normalized cross-correlation coefficient of  $0.99$ .

Interestingly, the slight hydrograph modification that does occur results in a discharge peak that is higher than the total recharge peak, as water that backed up into the infeeder is released near the time of peak discharge.

If we increase the infeeder reservoir area from  $A_{R,in} = 100 \text{ m}^2$  to  $A_{R,in} = 5000 \text{ m}^2$ , this increases the infeeder response time by a factor of  $50$ , so that  $\gamma_{in} \gg 1$ . The response of this system is notably different (Fig. 10c and d). Large quantities of water reverse into the infeeder, because it cannot equilibrate quickly. Long after the recharge pulse, the infeeder reservoir continues to drain the water that accumulated there. For this case, the junction interaction results not only in a broader discharge curve, but also a complex shape that is a function of the system geometry. Here, the normalized cross-correlation coefficient has dropped to  $0.84$ .

The analysis here suggests that there is a significant set of arborescent reservoir–constriction networks, where reservoir surface areas are modest and hydraulic response times are consequently short, for which the simple response time approach also applies, without any correction for the dynamics of junctions. Notably, our first example case seems much closer to a typical alpine glacier than the second case, which has a large reservoir ( $5000 \text{ m}^2$ ) feeding the infeeder. Additionally, infeeder response time provides a tool for estimating whether junction effects are likely to be important for a particular system geometry.

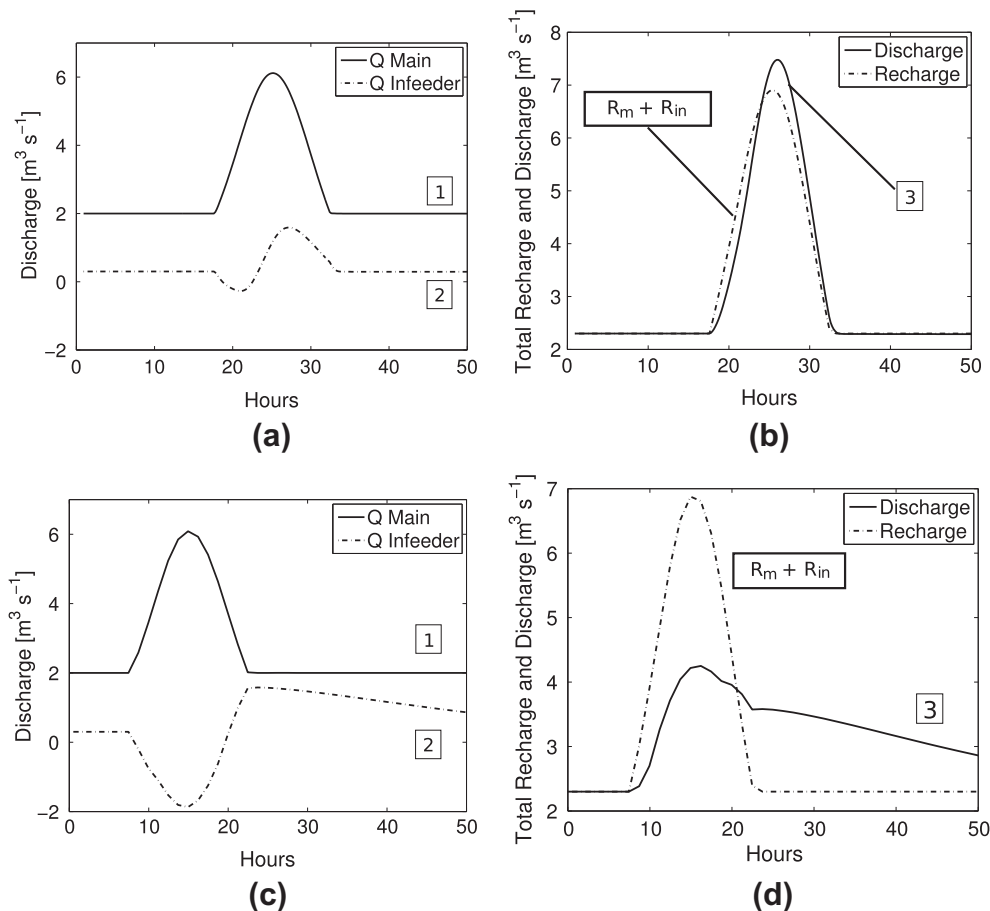


**Fig. 10.** Hydrographs for arborescent example cases. For panels a and b, the infeeder has a smaller reservoir surface area, with  $A_{R,in} = 100 \text{ m}^2$ . For panels c and d, the infeeder has a larger reservoir surface area, with  $A_{R,in} = 5000 \text{ m}^2$ . Panels a and c depict discharge through the main conduit above the junction (solid) and the infeeder (dashed). Panels b and d depict the total recharge (dashed) and discharge (solid) hydrographs. In both cases, hydraulic damping of the infeeder occurs, but it is much more significant for the simulation with a large infeeder reservoir. For the small reservoir case, the infeeder has little effect on the total discharge hydrograph (b) because the infeeder response time is shorter than the time scale for changes in recharge. For the large reservoir case (d), the discharge hydrograph is significantly modified by the infeeder because the infeeder response time is longer than the time scale for changes in recharge, and the infeeder also has a significant flow capacity. Locations of flow measurements noted in boxed labels are depicted in Fig. 9.

## 5.2. Linked-cavity flow systems

During the winter and early spring, when recharge rates are low, it is thought that subglacial flow occurs primarily through a distributed network, such as a system of linked-cavities (Walder, 1986; Kamb, 1987), extensive subglacial films (Weertman, 1972; Walder and Hallet, 1979; Sharp et al., 1990), or a porous medium at the base of the glacier (Fountain, 1994; Hubbard et al., 1995). Since such a flow system typically consists of a broad network of interconnected flow paths, it is quite different from the simple systems considered in Section 4, or the arborescent systems considered in Section 5.1. However, we show here that the single-element approach can be modified to approximate distributed flow in the linked-cavity case. A similar approach may be possible for other types of distributed systems, though we do not explore that in detail here.

For linked-cavities most of the head loss occurs within orifices (Walder, 1986) and the linked-cavity model can be conceptualized as a two-dimensional network of pipes, where each pipe represents a small orifice connecting two adjacent cavities. Kamb (1987) made this assumption when he calculated the total discharge of the linked-cavity system by summing over all of the independent flow paths across a transect of the glacier, and Arnold et al. (1998) use a similar approach of many small diameter parallel pipes to represent a distributed flow system.

Assuming that the input point is well-connected to the linked-cavity system, and the glacier is much longer than it is wide, so that the longitudinal gradients in hydraulic head are much larger than the transverse gradients, we can use the same approximation of many parallel pipes that was used by Kamb (1987) and Arnold et al. (1998). To extend the single-element model described above, we calculate the flow through parallel pipes connected to a single reservoir input point such as a moulin or crevasse (Fig. 11). Discharge through such a system is given by

$$Q_{\text{cav}} = N_0 A_0 \sqrt{\frac{2g}{C_{f,0}} (h_{\text{in}} - h_{\text{out}})}, \quad (12)$$

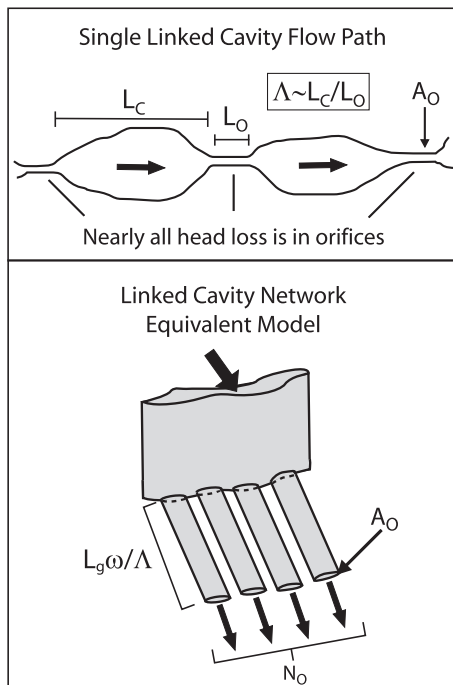


**Fig. 11.** The flow model that we use to represent a linked-cavity flow system. Recharge enters through a crevasse or moulin and is channeled into  $N_0$  different constricted pipes with cross-sectional areas  $A_0$ . The head loss is assumed to occur primarily in the constrictions so that each pipe has an equivalent length of  $L_g \omega / \Delta$ .

where  $N_0$  is the number of independent orifices (or flow routes),  $A_0$  is the typical orifice cross-sectional area,  $h_{\text{in}}$  is the hydraulic head at the input point, and  $h_{\text{out}}$  is the hydraulic head at the downstream end of the glacier.  $C_{f,0} = 1 + f L_g \omega / (\Delta D_{H,0})$  is a modified friction factor, where  $D_{H,0}$  is a typical orifice hydraulic diameter,  $\Delta \sim L_c / L_0$  is head gradient concentration factor, which is roughly equivalent to the ratio of typical cavity lengths,  $L_c$ , and orifice lengths,  $L_0$ , when  $L_c \gg L_0$ ,  $\omega$  is the flow path tortuosity, and  $L_g$  is the straight-line distance from the recharge point to the snout of the glacier.

If the linked-cavity flow Eq. (12) is substituted for the single pipe flow equation in the derivation of reservoir-constriction response time, we obtain a response time for a reservoir connected to a linked-cavity flow system,

$$\tau_{\text{cav}} = \frac{A_R C_{f,0} R_{\text{peak}}}{2g N_0^2 A_0^2} \approx \frac{A_R f L_g \omega R_{\text{peak}}}{2g N_0^2 \Delta D_{H,0} A_0^2}. \quad (13)$$

Here the reservoir area  $A_R$  can represent the surface area at a single input point that feeds many parallel flow paths, or the sum of areas at a number of input points that feed the parallel flow paths. So long as the area is partitioned evenly between flow paths, the equations for these two physical systems are the same. For realistic cases, the sum of all constriction lengths in a flow path will be much greater than the typical hydraulic diameter of an orifice, and then the approximation on the right of Eq. (13) holds. If we approximate the orifice geometry as rectangular, with a width,  $W_0$ , much larger than the height,  $H_0$ . Then Eq. (13) becomes

$$\tau_{\text{cav}} = \frac{A_R f L_g \omega R_{\text{peak}}}{4g N_0^2 \Delta H_0^3 W_0^2}. \quad (14)$$

Therefore, the linked-cavity response time is most strongly dependent upon the height of the orifices, and then on the orifice number and width.

As for the single flow path reservoir-constrictions, we run a set of 500 randomly generated linked-cavity flow simulations. For model parameters we use the ranges in Table 2 with the following additions:  $0.1 \text{ m} < W_0 < 3 \text{ m}$ ,  $0.01 \text{ m} < H_0 < 0.2 \text{ m}$ ,  $2 < N_0 < 20$ ,  $1 < \omega < 4$ ,  $5 < \Delta < 10$ . We further require that the orifices be low and wide, with  $H_0 / W_0 < 0.1$ , and orifice width is held constant throughout each simulation (i.e. melting and creep are only applied to the ceiling).

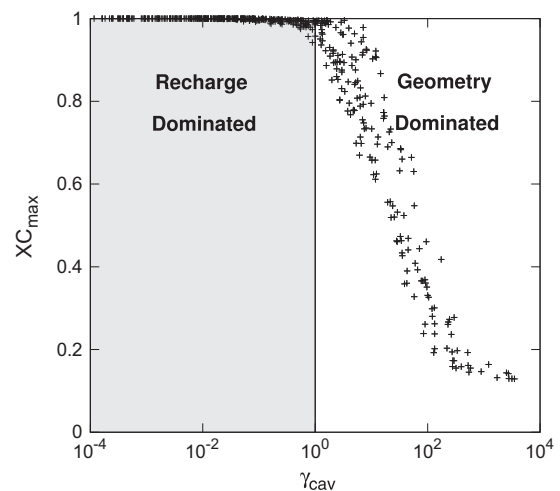


**Fig. 12.** Plot of the distribution of the maximum of the cross-correlation between recharge and discharge ( $XC_{\text{max}}$ ) versus the dimensionless number,  $\gamma_{\text{cav}}$ , for the randomly chosen linked-cavity reservoir-constriction simulations, depicted in Fig. 11. As for the single flow path reservoir-constrictions (Fig. 4), a critical value of  $\gamma = 1$  divides those cases where recharge or geometry is a dominant control of the discharge hydrograph.

We begin each simulation with a short equilibration period. If this is not done, we find that essentially all of the systems are recharge-dominated, and therefore it is difficult to verify the validity of the response time specified by Eq. (13). This suggests that, despite the relatively small orifice sizes, which are even smaller than the range listed above due to the equilibration period, the linked-cavity networks are more recharge-dominated than single conduits for the parameter distributions we have sampled for each system type. Fig. 12 shows that a modified form of  $\gamma$ , which uses the response time from Eq. (14), can be used to characterize the recharge–discharge responses of linked-cavity flow systems. The derived response time holds for systems that can be represented as parallel pipes (Fig. 11).

## 6. Do sharply-peaked hydrographs imply a channelized subglacial drainage system?

During the course of a melt season, proglacial hydrographs typically become narrower and more sharply peaked with shorter lags between peak melt and discharge (Fountain, 1992, 1996; Nienow

et al., 1998; Hannah et al., 1999; Willis et al., 2002; Swift et al., 2005; Bartholomew et al., 2011). Fountain (1992) argues that these effects are largely the result of evolution and removal of the snow-pack. However, authors continue to discuss the possibility that they are due to changes in the subglacial drainage system (Raymond et al., 1995; Swift et al., 2005; Jobard and Dzikowski, 2006; Flowers, 2008). Furthermore, snow pack removal and conduit development are thought to occur concurrently, as sharply peaked recharge input from bare portions of the glacier surface provide a likely mechanism for enlarging conduits and destabilizing a distributed flow network (Nienow et al., 1998). A relevant question is whether such peaked proglacial hydrographs require the presence of a well-developed conduit network. That is, will a distributed network always modulate sharply peaked recharge hydrographs to produce broader proglacial hydrographs, or will these peaked hydrographs sometimes pass through the system unchanged?

Within the simulation set above, where linked-cavity system parameters were chosen within a reasonable range, a large number of models are recharge-dominated and therefore do not modulate their recharge signals. We illustrate this point with two example flow geometries, one a single conduit and one a linked-cavity system. For each example geometry we simulate the response with two different recharge hydrographs. One is a broad, low peak hydrograph representative of muted recharge in the presence of snow cover ( $\sigma = 9$  h and  $R_{\text{peak}}/R_{\text{base}} = 1.5$ ). The other is a narrower, higher peak hydrograph representing recharge after the removal of snow ( $\sigma = 3$  h and  $R_{\text{peak}}/R_{\text{base}} = 3.0$ ).

Both example systems are started with conduit (or orifice) dimensions near equilibrium for a base recharge of  $0.15 \text{ m}^3 \text{ s}^{-1}$  and ice thickness of 200 m. The initial conduit diameter is 0.5 m, and initial orifice height is 0.05 m. A constant orifice width of 0.2 m is assumed, and we use values of  $N_0 = 25$ ,  $\omega = 4$ , and  $A = 10$ . For both systems,  $L = 2000$  m,  $A_R = 10 \text{ m}^2$ , and  $f = 0.1$ . These systems could be considered fairly typical for a conduit or linked-cavity network fed via a crevasse or large moulin, yet neither of them significantly modifies its recharge hydrograph (Fig. 13). In fact, the responses of the conduit and linked-cavity network are strikingly similar. In physical terms, neither example system is able to significantly change its storage volume during the recharge pulse. Therefore sharply-peaked discharge hydrographs that occur following the removal of the snowpack are not conclusive evidence that a channelized flow system is indeed present, because at least some types of distributed flow systems, such as a linked-cavity network, can display recharge-dominated behavior.

## 7. Discussion and conclusions

Proglacial hydrographs are known to evolve throughout the season. However, there is no broad agreement about the extent to which these hydrographs can be modulated by englacial and subglacial hydrological systems (Fountain, 1992, 1996; Nienow et al., 1998; Hannah et al., 1999; Swift et al., 2005; Jobard and Dzikowski, 2006; Flowers, 2008). We have employed a tool, the hydraulic response time, that quantitatively connects the geometry of a given conduit flow path with the ability of that flow path to influence hydrographs. In an analysis of single conduit flow paths, we find that the modulation of hydrographs by conduits is limited to cases where conduits are connected to larger storage volumes, such as crevasses and lakes, that can be filled and drained. We also find that linked-cavity systems, to the extent that they can be represented as a system of parallel pipes, are also unlikely to alter recharge hydrographs without the presence of large reservoirs. In order for system discharge hydrographs to differ significantly from recharge hydrographs, the system must have a

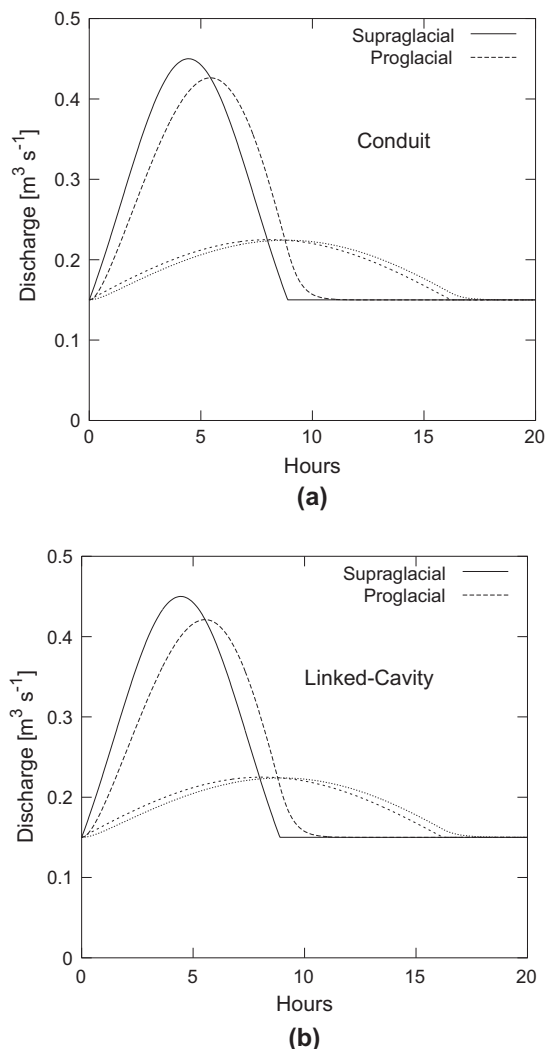


**Fig. 13.** Example supraglacial and proglacial hydrographs produced by typical conduit (a) and linked-cavity (b) systems, for both broad and sharp recharge hydrographs. For both types of systems, the broad proglacial and supraglacial hydrographs are barely distinguishable. The similarity of supraglacial and proglacial hydrographs suggests that many simple subglacial hydrological systems will not modify recharge hydrographs, and that peaked hydrographs are not a clear indicator of channelized flow.

changing storage volume that is significant compared to daily discharges. Our results suggest that the changing storage volume provided by the filling and draining of the conduits themselves is almost never significant in comparison to the discharge capacity of the conduits.

If our linked-cavity flow model captures the behavior of any real subglacial distributed systems, the example cases in Section 6 demonstrate that peaked hydrographs are not a clear indicator of the presence of a channelized conduit system. That is, some subset of distributed flow networks can transmit peaked recharge hydrographs. A porous medium simulation by Fountain (1992) of discharge through a subglacial debris layer demonstrates the transmission of sharply peaked hydrographs through a quite different type of distributed flow system, adding further support to our conclusion.

While some distributed systems will allow transmission of sharply peaked hydrographs, a wide variety of different types of distributed systems are thought to exist in nature, such as subglacial aquifers, permeable subglacial tills, thin films, and linked-cavities. The properties of each type of distributed flow system will also vary appreciably from one site to another. There are certainly ranges of this broad parameter space where distributed systems will exhibit sufficient changes in storage capacity over short enough time scales to produce significant modulation of diurnal melt pulses.

One complexity that we have not considered explicitly is the interactions between conduits and distributed flow systems that can drain and fill storage volumes within the till and at the ice-bed interface (Alley, 1992, 1996; Hubbard et al., 1995; Flowers, 2008). Simulations by Flowers (2008), which use a 1-dimensional model that couples conduits, a distributed flow system represented as a compressible porous medium, and a subglacial aquifer, show that the distributed network can have a significant effect on proglacial hydrographs. They note that glaciers coupled to more permeable substrates have more capacity to dampen the flood pulses propagating through the system. In these simulations, the distributed flow network is capable of damping the recharge curves because the volume of water stored in it is changing appreciably over diurnal time scales.

Ice dynamics can also play a role in hydrograph modification in some cases. During diurnal melt pulses, a glacier can be temporarily lifted from its bed in the vicinity of conduits, allowing periodic exchange of water between the conduit and voids created between ice and till (Stone and Clarke, 1993). Clarke (1996) modeled this process using a non-linear elastic reservoir, a model that might adapt itself to the type of analysis developed in this work. In cases where such volumes are sufficiently large in comparison to daily discharges, they could influence recharge–discharge relations. At a larger scale, draining lakes can result in significant uplift of the ice (Das et al., 2008; Shepherd et al., 2009), with correspondingly large storage volumes filling over short time scales.

An additional simplification of the models developed in this work is that they primarily consider the reservoir surface area and recharge associated with a single input point. Glacial hydrological systems will typically contain many input points with associated storage volumes and recharges. We have considered parameter ranges, for both surface area and recharge, that are appropriate for single inputs. Therefore, it seems possible that the calculation of  $\gamma$  could be extended to larger networks, either by calculating  $\gamma$  values for all major inputs and performing a discharge-weighted average, or by summing total reservoir areas and recharges over the entire system and using a representative conduit diameter. However, developing such an approach would require significant additional simulation work to verify the proper formulation.

The fundamental concepts that underlie our approach, hydraulic response time, recharge time scale, and changes in reservoir volume, can potentially be applied to investigate the recharge–discharge relations of other types of distributed flow systems and the effects of exchange of water between conduits and porous distributed flow systems or gaps at the ice-bed interface. Covington et al. (2009) provide a brief discussion of how porous medium response times can be derived, and this would be applicable to cases where recharge occurs directly into a porous medium distributed flow element. Exchange flows between conduits and other storage elements are analogous to the interactions that occur at conduit junctions, and similar techniques may apply. For example, a porous medium surrounding a conduit can be treated as a type of reservoir, and its ability to affect proglacial hydrographs will depend critically on the storage volume of the reservoir and the time scale over which it can fill and drain. In analogy with junctions in conduit systems, to modulate hydrographs, exchanges between storage elements and conduits during recharge pulses must be significant in comparison to the discharge through the conduit system. For storage elements that are saturated and relatively incompressible, as may often be the case with basal crevasses (Harper et al., 2010), the volume is essentially fixed and no hydrograph modification will occur.

Given the prevalence of recharge-dominated hydraulic responses, even in arborescent systems and our simplified model of a linked-cavity system, we conclude that sharply-peaked proglacial discharge hydrographs are unreliable indicators of a channelized conduit system, unless combined with an accurate account of glacial recharge. Similarly, dispersed hydrographs may not be indicative of a distributed subglacial flow system. In conclusion, proglacial hydrographs are controlled by a number of factors, including surface melt rates, surface routing, and subglacial routing. While the first two factors will always play an important role, subglacial processes influence the hydrograph to a varying degree, depending on the exact structure of the network. Since hydrographs can be strongly controlled by recharge, and, in turn, discharge is a first-order control over other proglacial signals such as chemographs and tracer breakthrough curves, quantifying recharge is crucial in future field studies of proglacial time series.

## Acknowledgments

M.D.C. is supported by a National Science Foundation (NSF) Earth Sciences Postdoctoral Fellowship (081647), A.B. by a Natural Environment Research Council Doctoral Training Grant, and J.G. by an NSF Earth Sciences Postdoctoral Fellowship (0946767). M.O.S. acknowledges the George and Orpha Gibson endowment of the Hydrogeology and Geofluids Research Group and support from NSF Grants DMS-0724560 and EAR-0941666. The comments of two anonymous reviewers helped to significantly improve the clarity and precision of the text.

## References

- Alley, R., 1992. How can low-pressure channels and deforming tills coexist subglacially? *J. Glaciol.* 38 (128).
- Alley, R.B., 1996. Towards a hydrological model for computerized ice-sheet simulations. *Hydrol. Process.* 10 (4), 649–660.
- Anderson, S.P., Walder, J.S., Anderson, R.S., Kraal, E.R., Cunico, M., Fountain, A.G., Trabant, D.C., 2003. Integrated hydrologic and hydrochemical observations of Hidden Creek Lake Jökulhlaups, Kennicott Glacier, Alaska. *J. Geophys. Res.* 108 (F1), 6003.
- Arnold, N., Richards, K., Willis, I., Sharp, M., 1998. Initial results from a distributed, physically based model of glacier hydrology. *Hydrol. Process.* 12, 191–219.
- Bartholomew, T., Anderson, R., Anderson, S., 2008. Response of glacier basal motion to transient water storage. *Nat. Geosci.* 1 (1), 33–37.
- Bartholomew, I., Nienow, P., Sole, A., Mair, D., Cowton, T., Palmer, S., Wadham, J., 2011. Supraglacial forcing of subglacial drainage in the ablation zone of the



- Greenland ice sheet. *Geophys. Res. Lett.* 38 (8), 1–5. doi:10.1029/2011GL047063.
- Bingham, R.G., Nienow, P.W., Sharp, M.J., 2003. Intra-annual and intra-seasonal flow dynamics of a high arctic polythermal valley glacier. *Ann. Glaciol.* 181–188 (8). doi:10.3189/172756403781815762.
- Boon, S., Sharp, M., 2003. The role of hydrologically-driven ice fracture in drainage system evolution on an Arctic glacier. *Geophys. Res. Lett.* 30 (18), 1916.
- Clarke, G.K.C., 1996. Lumped-element analysis of subglacial hydraulic circuits. *J. Geophys. Res.* 101, 17,547–17,560. doi:10.1029/96JB01508.
- Clarke, G., 2003. Hydraulics of subglacial outburst floods: new insights from the Spring–Hutter formulation. *J. Glaciol.* 49 (165), 299–313.
- Covington, M., Wicks, C., Saar, M., 2009. A dimensionless number describing the effects of recharge and geometry on discharge from simple karstic aquifers. *Water Resour. Res.* 45 (11), W11410. doi:10.1029/2009WR008004.
- Das, S.B., Joughin, I., Behn, M.D., Howat, I.M., King, M.A., Lizarralde, D., Bhatia, M.P., 2008. Fracture propagation to the base of the Greenland ice sheet during supraglacial lake drainage. *Science* 320, 778. doi:10.1126/science.1153360.
- Flowers, G., 2008. Subglacial modulation of the hydrograph from glacierized basins. *Hydrol. Process.* 22 (19), 3903–3918.
- Flowers, G., Clarke, G., 2002. A multicomponent coupled model of glacier hydrology: 1. Theory and synthetic examples. *J. Geophys. Res.* 107 (10.1029).
- Fountain, A., 1992. Subglacial water flow inferred from stream measurements at South Cascade Glacier, Washington, USA. *J. Glaciol.* 38, 128.
- Fountain, A., 1993. Geometry and flow conditions of subglacial water at South Cascade Glacier, Washington State, USA: an analysis of tracer injections. *J. Glaciol.* 39 (131), 143–156.
- Fountain, A., 1994. Borehole water-level variations and implications for the subglacial hydraulics of South Cascade Glacier, Washington State, USA. *J. Glaciol.* 40 (135).
- Fountain, A., 1996. Effect of snow and firn hydrology on the physical and chemical characteristics of glacial runoff. *Hydrol. Process.* 10 (4), 509–521.
- Fountain, A.G., Jacobel, R.W., Schlichting, R., Jansson, P., 2005. Fractures as the main pathways of water flow in temperate glaciers. *Nature* 433, 618–621.
- Fowler, A., 1987. Sliding with cavity formation. *J. Glaciol.* 33 (115), 255–267.
- Gulley, J., Benn, D., Muller, D., Luckman, A., 2009a. A cut-and-closure origin for englacial conduits in uncrevassed regions of polythermal glaciers. *J. Glaciol.* 55 (189), 66–80.
- Gulley, J.D., Benn, D.I., Screaton, E., Martin, J., 2009b. Mechanisms of englacial conduit formation and their implications for subglacial recharge. *Quaternary Sci. Rev.* 28 (19–20), 1984–1999. doi:10.1016/j.quascirev.2009.04.002.
- Gulley, J., Walthard, P., Martin, J., Banwell, A., Benn, D., Catania, G., Willis, I., submitted for publication. The effects of recharge and relative roughness of subglacial conduits on the velocity and dispersivity of dye traces in glaciers. *J. Glaciol.*
- Hannah, D.M., Gurnell, A.M., McGregor, G.R., 1999. A methodology for investigation of the seasonal evolution in proglacial hydrograph form. *Hydrol. Process.* 13 (16), 2603–2621.
- Harper, J., Bradford, J., Humphrey, N., Meierbachtol, T., 2010. Vertical extension of the subglacial drainage system into basal crevasses. *Nature* 467 (7315), 579–582.
- Hindmarsh, A., 1983. ODEPACK, a systematized collection of ODE solvers. In: Stepleman, R.e.a. (Ed.), *IMACS Transactions on Scientific Computation*, vol. 1. Scientific Computing, pp. 55–64.
- Hock, R., Hooke, R.L., 1993. Evolution of the internal drainage system in the lower part of the ablation area of Storglaciären, Sweden. *Bull. Geol. Soc. Am.* 105 (4), 537.
- Hubbard, B., Sharp, M., Willis, I., Nielsen, M., Smart, C., 1995. Borehole water-level variations and the structure of the subglacial hydrological system of Haut Glacier d'Arolla, Valais, Switzerland. *J. Glaciol.* 41 (139), 572–583.
- Jobard, S., Dzikowski, M., 2006. Evolution of glacial flow and drainage during the ablation season. *J. Hydrol.* 330 (3–4), 663–671.
- Kamb, B., 1987. Glacier surge mechanism based on linked cavity configuration of the basal water conduit system. *J. Geophys. Res.* 92, 9083–9100. doi:10.1029/JB092iB09p09083.
- Mair, D., Sharp, M., Willis, I., 2002. Evidence for basal cavity opening from analysis of surface uplift during a high-velocity event: Haut Glacier d'Arolla, Switzerland. *J. Glaciol.* 48 (161), 208–216.
- Murray, T., Stuart, G., Fry, M., Gamble, N., Crabtree, M., 2000. Englacial water distribution in a temperate glacier from surface and borehole radar velocity analysis. *J. Glaciol.* 46 (154), 389–398.
- Nienow, P.W., Sharp, M., Willis, I.C., 1996. Velocity–discharge relationships derived from dye tracer experiments in glacial meltwaters: implications for subglacial flow conditions. *Hydrol. Process.* 10, 1411–1426.
- Nienow, P.W., Sharp, M., Willis, I.C., 1998. Seasonal changes in the morphology of the subglacial drainage system, Haut Glacier d'Arolla, Switzerland. *Earth Surf. Process. Landforms* 23, 825–843.
- Raymond, C., Benedict, R., Harrison, W., Echelmeyer, K., Sturm, M., 1995. Hydrological discharges and motion of Fels and Black Rapids Glaciers, Alaska, USA: implications for the structure of their drainage systems. *J. Glaciol.* 41 (138), 290–304.
- Röthlisberger, H., 1972. Water pressure in intra- and subglacial channels. *J. Glaciol.* 11 (62), 177–203.
- Schoof, C., 2010. Ice-sheet acceleration driven by melt supply variability. *Nature* 468 (7325), 803–806. doi:10.1038/nature09618.
- Schuler, T.V., Fischer, U.H., 2009. Modeling the diurnal variation of tracer transit velocity through a subglacial channel. *J. Geophys. Res.* 114, F04017.
- Schuler, T., Fischer, U., Gudmundsson, G., 2004. Diurnal variability of subglacial drainage conditions as revealed by tracer experiments. *J. Geophys. Res.* 109, F02008.
- Sharp, M., Tison, J., Fierens, G., 1990. Geochemistry of subglacial calcites: implications for the hydrology of the basal water film. *Arctic Alpine Res.* 22 (2), 141–152.
- Shepherd, A., Hubbard, A., Nienow, P., King, M., McMillan, M., Joughin, I., 2009. Greenland ice sheet motion coupled with daily melting in late summer. *Geophys. Res. Lett.* 36 (1), L01501.
- Shreve, R., 1972. Movement of water in glaciers. *J. Glaciol.* 11 (62), 205–214.
- Smart, C., 1990. Comments on Character of the englacial and subglacial drainage system in the lower part of the ablation area of Storglaciären, Sweden, as revealed by dye-trace studies. *J. Glaciol.* 36, 126–128.
- Spring, U., Hutter, K., 1981. Numerical studies of Jökulhlaups. *Cold Regions Sci. Technol.* 4 (3), 221–244.
- Stone, D., Clarke, G., 1993. Estimation of subglacial hydraulic properties from induced changes in basal water pressure: a theoretical framework for borehole-response tests. *J. Glaciol.* 39, 327–340.
- Sugiyama, S., Naruse, R., Murav'yev, Y., 2005. Surface strain anomaly induced by the storage and drainage of englacial water in Koryto glacier, Kamchatka, Russia. *Ann. Glaciol.* 40 (1), 232–236.
- Swift, D.A., Nienow, P.W., Hoey, T.B., Mair, D.W.F., 2005. Seasonal evolution of runoff from Haut Glacier d'Arolla, Switzerland and implications for glacial geomorphic processes. *J. Hydrol.* 309.
- Tranter, M., Brown, G.H., Hodson, A.J., Gurnell, A.M., 1996. Hydrochemistry as an indicator of subglacial drainage system structure: a comparison of Alpine and sub-Polar environments. *Hydrol. Process.* 10 (4), 541–556.
- Walder, J.S., 1986. Hydraulics of subglacial cavities. *J. Glaciol.* 32, 439–445.
- Walder, J., Fowler, A., 1994. Channelized subglacial drainage over a deformable bed. *J. Glaciol.* 40 (134), 3–15.
- Walder, J., Hallet, B., 1979. Geometry of former subglacial water channels and cavities. *J. Glaciol.* 23 (89), 335–346.
- Weertman, J., 1972. General theory of water flow at the base of a glacier or ice sheet. *Rev. Geophys.* 10 (1), 287–333.
- Werder, M., Schuler, T., Funk, M., 2010a. Short term variations of tracer transit speed on Alpine glaciers. *The Cryosphere* 4, 381–396.
- Werder, M., Schuler, T.V., Funk, M., 2010b. Short term variations of tracer transit speed on alpine glaciers. *The Cryosphere* 4 (3), 381–396. doi:10.5194/tc-4-381-2010.
- Willis, I.C., 1995. Intra-annual variations in glacier motion, a review. *Prog. Phys. Geogr.* 19.
- Willis, I.C., Sharp, M.J., Richards, K.S., 1990. Configuration of the drainage system of Midtdalsbreen, Norway, as indicated by dye-tracing experiments. *J. Glaciol.* 36 (122).
- Willis, I., Arnold, N., Brock, B., 2002. Effect of snowpack removal on energy balance, melt and runoff in a small supraglacial catchment. *Hydrol. Process.* 16 (14), 2721–2749.